The transcriptome of the mosquito host *Anopheles gambiae* upon infection by different selected lines of the microsporidian parasite *Vavraia culicis*

Luís M. Silva [1,2] *

[1] Institute of Biology, University of Neuchâtel, Rue Emilie-Argand 11, 2000 Neuchâtel, Switzerland

[2] Department of Zoology, University of British Columbia, 6270 University Boulevard, Vancouver, BC V6T 1Z4, Canada

* Corresponding author: luis.silva@ubc.ca

ORCID

LMS: 0000-0002-8203-4006

Abstract (198)

Understanding host-parasite interactions is of the utmost importance for disease prediction, prevention and management. Hence, this study assessed the transcriptional response of the primary malaria vector, *Anopheles gambiae*, to infection with several lines of the candidate vector-control parasite, the microsporidian *Vavraia culicis*. These parasitic lines were selected for early or late transmission within this host. Previous studies extensively described them phenotypically, differing in their virulence, infection dynamics and host exploitation. Using RNA sequencing, gene expression profiles were analyzed in *Anopheles gambiae* mosquitoes infected with early-transmission-selected, late-transmission-selected, unselected (*Stock*) *V. culicis* lines and uninfected controls. The results revealed distinct transcriptional changes associated with each parasite line. Early-selected parasites induced a broader immune response than late-selected ones. Differential expression of immune-related genes, including *Toll-interacting protein* and *Protein ERGIC-53* was identified. Additionally, significant changes were observed in pathways related to Golgi membrane function and oxidative stress response, particularly in response to early-selected parasites. These findings highlight the evolutionary pressures shaping host-parasite coevolution and provide insights into how parasite transmission traits can influence mosquito immune response and regulation. This work offers a foundation for future studies on mosquito-microsporidia dynamics and potential applications for vector control strategies, particularly with respect to *Plasmodium* control.

Background (1190)

Mosquitoes encounter numerous parasites throughout their life cycle [1–6]. Among them, one fungal phylum has drawn significant attention from vector biologists due to its potential as a biological control agent against vector-borne diseases [7–9]. This group, Microsporidia, consists of unicellular intracellular parasites that infect a wide range of organisms, from honeybees to humans, and span diverse ecological niches, including soil and aquatic environments [7, 10–14].

Microsporidian species that infect mosquitoes are predominantly aquatic, as they are adapted to target mosquito larvae that feed in water bodies. The most extensively studied species in this group is *Vavraia culicis* (Order: Glugeida, Family: Pleistophoridae). Like other mosquito-infecting microsporidia, *V. culicis* reaches the gut after ingestion, integrating the host gut cells along the extracellular matrix [15]. A key feature of microsporidian spores facilitates this process: the polar tube. This harpoon-like, protein-based apparatus, typically coiled within the spore, enables the parasite to inject the sporoplasm (containing all genetic material) directly into the host cell and start parasite replication. Once the infected cell reaches its maximum capacity of spores, it lyses, releasing the newly formed spores. In *V. culicis*, this cycle repeats multiple times in the gut, followed by the fat

body. These spores will get transmitted into a new host through one of two ways: horizontal transmission, in mosquitoes that die on water, release the spores, which infect nearby larvae and restart the infection cycle; Transovum (vertical) transmission, where the laid eggs are covered in spores and infect other larvae either through cannibalism or contamination of the water body [15].

In a time where strategies to control the public health toll of vector-borne diseases are starting to come short in efficiency, microsporidian parasites offer a possible solution [7, 8, 16, 17], in particular *V. culicis*, with its ease of culture in the lab [18–21] and potentially Microsporidia MB [8, 22]. Several studies have demonstrated that co-infection with *V. culicis* impairs *Plasmodium spp.* (i.e., malaria-causing parasite) development within its mosquito vectors, *Anopheles spp.*, and the same has been hypothesized to vector-borne diseases carried by *Aedes aegypti* (e.g., dengue) [23]. Besides this, *V. culicis* also has been shown to improve the efficiency of insecticides against mosquitoes via restoration of their sensibility to insecticides [16]. Since *V. culicis* is not cleared by *Anopheles* mosquitoes [24], maintaining its prevalence in mosquito populations. Although a lot has been done to understand infection by *V. culicis* in *Anopheles* mosquitoes [20, 24–29], research has fallen short on describing the molecular mechanisms and pathways involved in the infection and response to this parasite, let alone the underpinnings of its *Plasmodium*-inhibitory effect.

When we consider mosquito infections with *Plasmodium spp.,* we cannot disregard the fact that this parasite can only be transmitted in mosquitoes that live long enough for the parasite to develop (e.g., approximately 20 days for *Plasmodium berghei*). Hence, this setting might also select for co-infecting parasites that can survive this long within the host. In the case of *V. culicis* a short or a long time within the host might affect its *Plasmodium*-inhibitory potential. Moreover, despite their small genome [14, 28, 30], which could hinder the number of genes where mutation can happen, *V. culicis* has been shown to evolve rapidly [25]. Taking this into consideration, Silva and Koella (2024) artificially selected *V. culicis* that: i) killed the host *Anopheles gambiae* (Order: Diptera, Family: Culicidae) faster and therefore spent less time within it (host death and release of spores approximately at 1 to 7 days of adulthood, hereafter *Early* regime); or ii) allowed the host to live longer and therefore remained in its system for longer too (host death and release of spores approximately at 20 to 30 days of adulthood, hereafter *Late* regime). Surprisingly, they found more time within the host selected the parasite lines of *V. culicis* to be more virulent (i.e., mosquitoes infected with *Late* parasites had a mean time to death of 15.31 ± 0.22 days; *Early* 18.17 ± 0.01; and *Stock* 20.31 ± 0.56), faster parasite development, and higher spore burdens (for day 10 of adulthood: *Late* with 239,500 ± 23,352; *Early* with 98,080 ± 14,853; and *Stock* with 78,900 ± 11,919 spores per mosquito) to throughout their life (which will reflect in higher transmission rates upon death), when compared to lines selected to spend less time within their host, or the unselected stock laboratory population of the parasite (hereafter referred to as *Stock*) [25]. These findings reinforce the potential of this microsporidian species as a biological control agent, as higher replication of *V. culicis* in long-

lived mosquitoes might increase its *Plasmodium*-inhibitory effect. The potential increase of the inhibitory effect is due to the two main hypotheses for how the inhibitory process takes place, which are resource competition or collateral immune response, both of which are parasite growth-dependent.

Thus, in this study, I aimed to characterize the response of the host *A. gambiae* to infection with unselected and selected lines of *V. culicis* through RNA-sequencing (RNA-seq). With this approach, I had two main aims: i) describe the host response to the unselected *Stock* population of *V. culicis*; and ii) compare the host response to five *Early* from five *Late* selected lines of *V. culicis* obtained from Silva and Koella (2024) (Fig. 1). Through the inclusion of these selected lines, variability in parasite treatments was increased, which may provide insights into which expression patterns are more readily available or likely to evolve in response to different parasite challenges. An uninfected mosquito treatment (hereafter *Uninfected)* was also included as a baseline for the *Stock*-infected mosquito treatment. The time-point selected to assess their transcriptome was day 10 of adulthood for two reasons: i) previous results have shown all infected mosquitoes, regardless of the parasite treatment, are actively releasing infective spores in high numbers, and therefore most likely to induce a host response that can be detected; ii) an assessment of the host response during the early stages of infection is more likely to show clear differences between the parasites, which would be more informative. When considering host immunity, mosquitoes do not possess an adaptive immune system, and instead their immune defences are mediated by innate immunity, with critical pathways, such as the Toll, Imd and JAK-STAT pathways, involved in parasite recognition and elimination [31, 32].

The findings of this study provide the first insights into the *A. gambiae* transcriptional response to infection by *V. culicis*, while also demonstrating how parasite evolution drives changes in genome expression, impacting the ability of the mosquito to respond to infection. Such insights have been performed in *Aedes aegypti,* a vector of dengue, unveiling a weak immune response, but significant up-regulation in lectins and CLIP-domain serine proteases [33], both effectors involved in innate immunity and its signalling [34]. This study complements previous work on these *V. culicis* lines, providing a more comprehensive understanding of this host-parasite interaction. Moreover, the data presented here have important implications for a more general understanding of parasite fitness, as well as mosquito vector competence for vector-borne parasites. Understanding the molecular basis of interactions is crucial for designing effective vector control strategies that exploit the natural evolutionary pressures acting on mosquito-parasite systems [35].

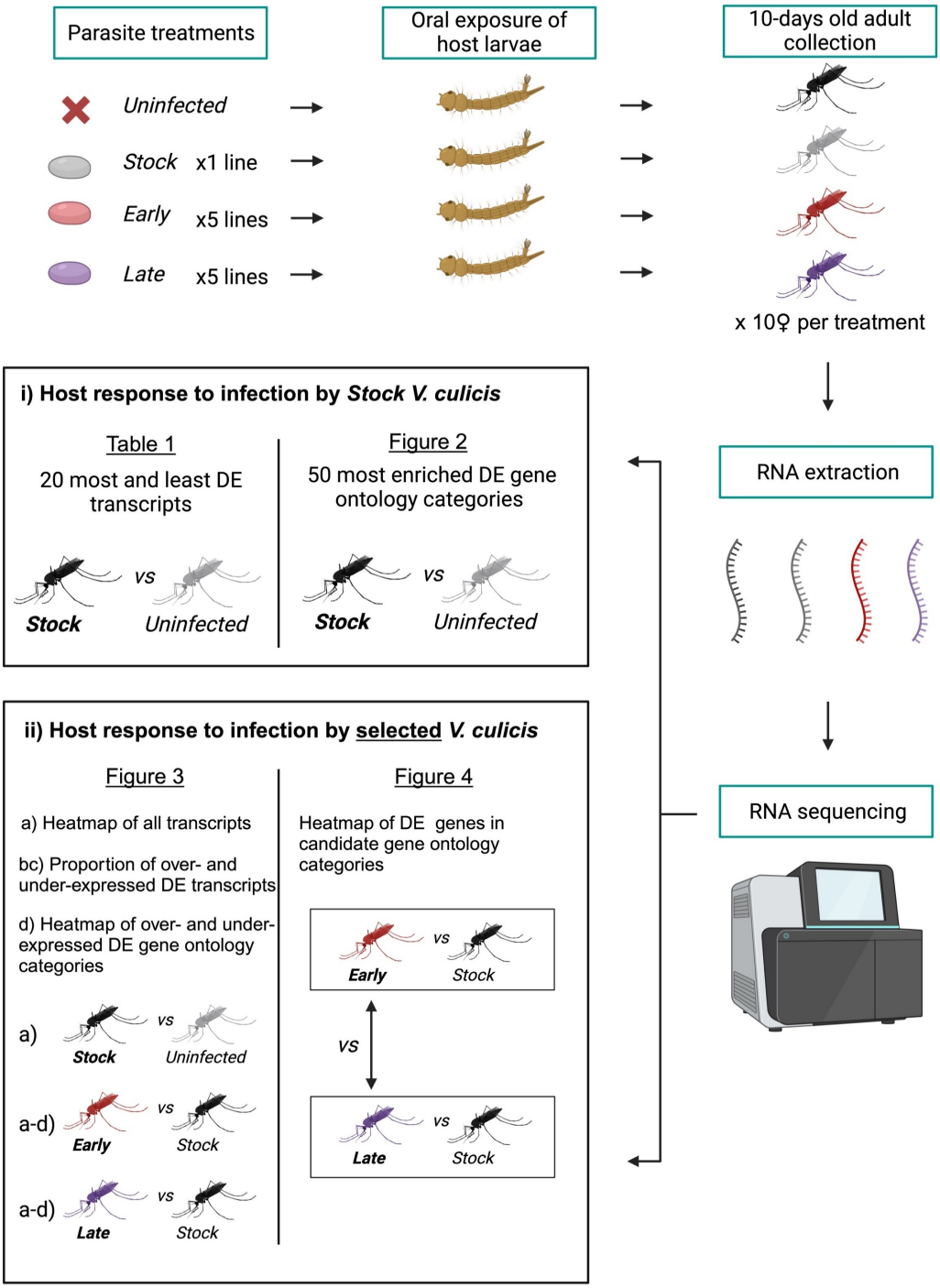

Figure 1. Illustration of the experimental workflow and results. Naive *Anopheles gambiae* mosquito larvae were either uninfected or infected with one of three different sets of lines of the parasite *Vavraia culicis,* to create the following four experimental groups: (1) uninfected mosquitoes (*Uninfected*); (2) mosquitoes infected with spores from an unselected *V. culicis* line (*Stock*); (3) mosquitoes infected with spores from a *V. culicis* line previously selected for early transmission from mosquito hosts (*Early*); and (4) mosquitoes infected with spores from a *V. culicis* line previously selected for late transmission from mosquito hosts (*Late*). After larval infection and subsequent

134 pupation, adult mosquitoes were collected at day 10 post-adult-emergence and pooled to create 10
135 individuals per selection replicate for RNA extraction (10 females x 5 selection replicates). Then,
136 differences in host response to the presence/absence of the parasite were assessed. First, the 20 most
137 and least expressed transcripts in *Stock*-infected mosquitoes, comparatively to *Uninfected* (Table 1),
138 were identified, as well as the most represented gene ontology (GO) categories and the proportion of
139 genes DE (Fig. 2). Second, all DE transcripts were presented according to their respective (GO)
140 biological process. The latter was followed by a heatmap of the GO categories that are
141 upregulated/downregulated in infection by the *Early* and *Late* parasites, comparatively to the *Stock*
142 parasite (Fig. 3). Third, selected candidate GO categories from Figure 3 that differed the most
143 between *Early* and *Late* were compared. The expression of the transcripts from these categories was
144 then tested for differences between selection regimes (Fig. 4).

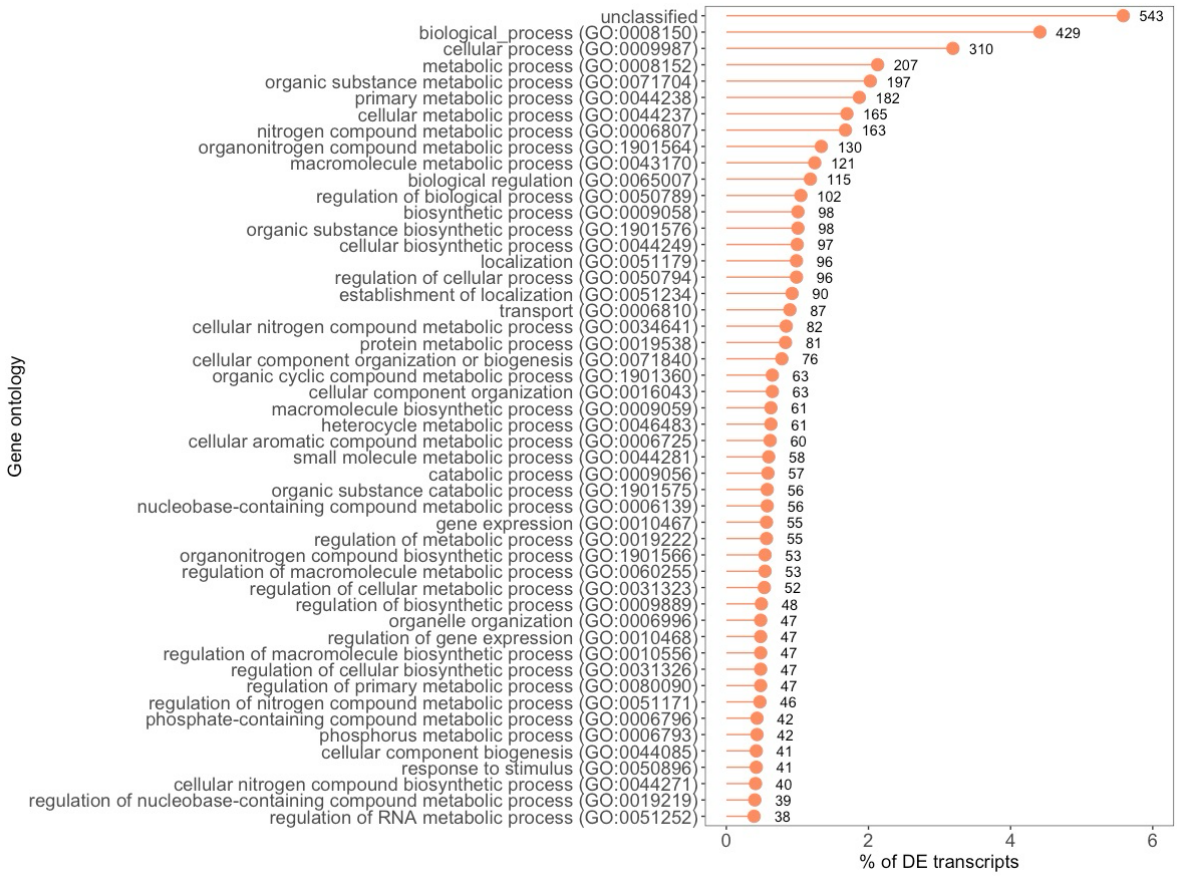

145

146 **Figure 2. Most enriched gene ontology categories in infected mosquitoes compared to**
147 **uninfected.** Percentage of differentially expressed (DE) transcripts in *A. gambiae* infected with *Stock*
148 *V. culicis,* comparatively to *Uninfected* hosts. The plot shows the 50 most enriched gene ontology
149 categories, the percentage of DE transcripts per category, and the absolute number of transcripts (on
150 the right to each dot).

151

152 **Table 1. Most up-and down-regulated genes in mosquitoes upon infection with the *Stock V.***
153 ***culicis* parasite compared to *Uninfected*.** The host transcriptomic profile concerning an unselected
154 *Stock V. culicis* parasite during infection was compared to the uninfected host profile. The 20
155 transcripts with the highest and lowest expression, compared to the control, are presented. Fold
156 change and *p*-value were calculated using the transcriptional expression of four technical replicates
157 per treatment. See materials and methods for more details. The *p*-value was adjusted using the
158 Benjamini-Hochberg correction method for each comparison, controlling for a false discovery rate (p
159 < 0.05).

#	Gene ID	Gene name	Fold change	Adj. *p*
1	LOC3291958	Putative uncharacterized protein DDB_G0271606	-1680.95	< 0.001
2	LOC133393242	Uncharacterized	-306.13	< 0.001
3	LOC1281554	Protein CIMAP1D	-250.60	< 0.001
4	LOC1271479	Uncharacterized	-246.11	< 0.001
5	LOC133393316	Uncharacterized	-195.71	< 0.001
6	LOC1281083	Arginine kinase 1	-191.24	< 0.001
7	LOC1273786	Serine/arginine-rich splicing factor 2	-190.72	< 0.001
8	LOC133394019	Nucleosome assembly protein 1-like 1	-164.62	< 0.001
9	LOC133391046	Putative cyclin-dependent serine/threonine-protein kinase DDB_G0272797/DDB_G0274007	-161.63	< 0.001
10	LOC1271272	Uncharacterized	-149.47	< 0.001
11	LOC5667228	Uncharacterized	-133.19	< 0.001
12	LOC1269550	Uncharacterized	-126.11	< 0.001
13	LOC1270351	Uncharacterized	-123.92	< 0.001
14	LOC133391930	Uncharacterized	-121.19	< 0.001
15	LOC1277465	Uncharacterized	-119.77	< 0.001
16	LOC133391419	Uncharacterized	-107.89	< 0.001
17	LOC11175695	Uncharacterized	-107.77	< 0.001
18	LOC1278052	Cytosol aminopeptidase	-103.75	< 0.001
19	LOC1267823	Uncharacterized	-95.91	< 0.001
20	LOC4576455	Dynein regulatory complex subunit 4	-89.14	< 0.001
1	LOC1281665	Uncharacterized	13.30	< 0.001
2	LOC1269260	Stress-activated protein kinase JNK	4.89	< 0.001
3	LOC1280522	Neuropeptide FF receptor 2	4.40	0.039
4	LOC4576208	Protein obstructor-E	4.15	< 0.001
5	LOC1271120	Protein regulator of cytokinesis 1	4.10	< 0.001
6	LOC1279262	CLIP domain-containing serine protease B15	4.10	< 0.001
7	LOC1269964	Chymotrypsin-2-like	3.99	0.007
8	LOC1270108	Uncharacterized	3.97	0.020
9	LOC1281383	Ninjurin-2	3.96	0.002
10	LOC1279267	CLIP domain-containing serine protease B15-like	3.89	0.002
11	LOC1277042	Uncharacterized	3.76	< 0.001
12	LOC133392142	Uncharacterized	3.62	0.030
13	LOC1271472	Uncharacterized	3.62	< 0.001
14	LOC4577422	Uncharacterized	3.43	< 0.001
15	LOC133393335	Uncharacterized	3.39	0.005
16	LOC133393411	Uncharacterized	3.33	0.001
17	LOC1280050	Annulin	3.27	< 0.001

18	LOC1269628	Monocarboxylate transporter 12	3.27	0.011
19	LOC1271676	Uncharacterized	3.18	< 0.001
20	LOC1277959	UDP-glucosyltransferase 2	3.12	< 0.001

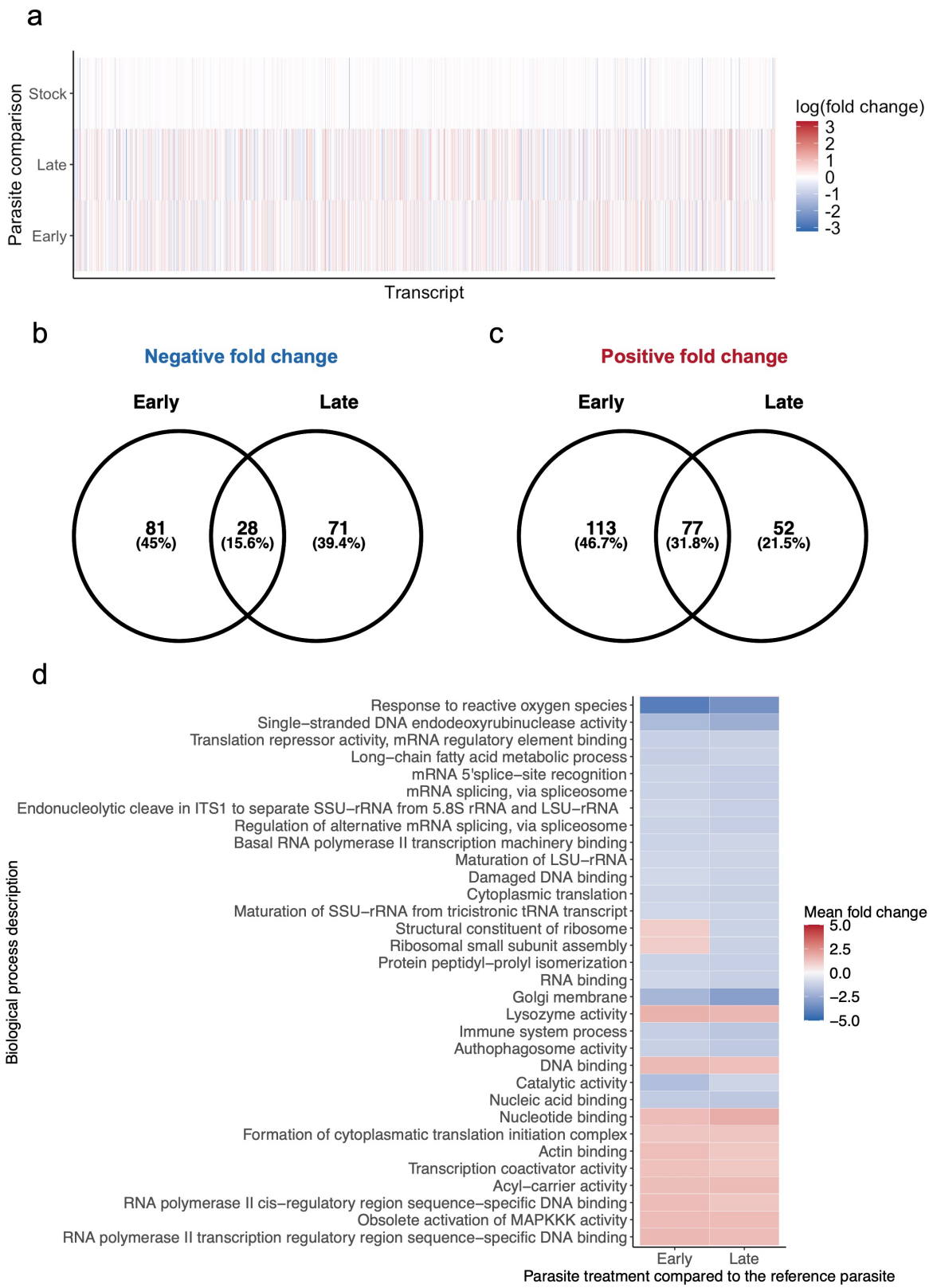

162

163 **Figure 3. Host transcriptional signatures of infection. (a)** Heatmap showing the log-transformed
164 fold change in expression of all detected transcripts (i.e., 9920) by parasite treatment comparison.
165 While the host transcriptome in response to the *Stock* parasite was compared to the *Uninfected* host
166 transcriptome, the response to *Early* and *Late* parasite treatments was compared to the response to the
167 *Stock* parasite. A heatmap of all biological samples can be found in SI Figure S3. **(bc)** Venn diagrams
168 showing the number of differentially expressed (DE) genes (adjusted p-value < 0.05) exclusively and
169 commonly found between hosts infected with *Early* or *Late* parasites in comparison to the *Stock*
170 parasite. Negative (b) and positive (c) differential expression are presented. (d) Heatmap illustrating
171 mean fold change in expression per biological processes families of significantly DE transcripts
172 across all replicates of the same selection regime. Gene ontology annotation was performed using
173 PANTHER 19.0 and VectorBase.

174

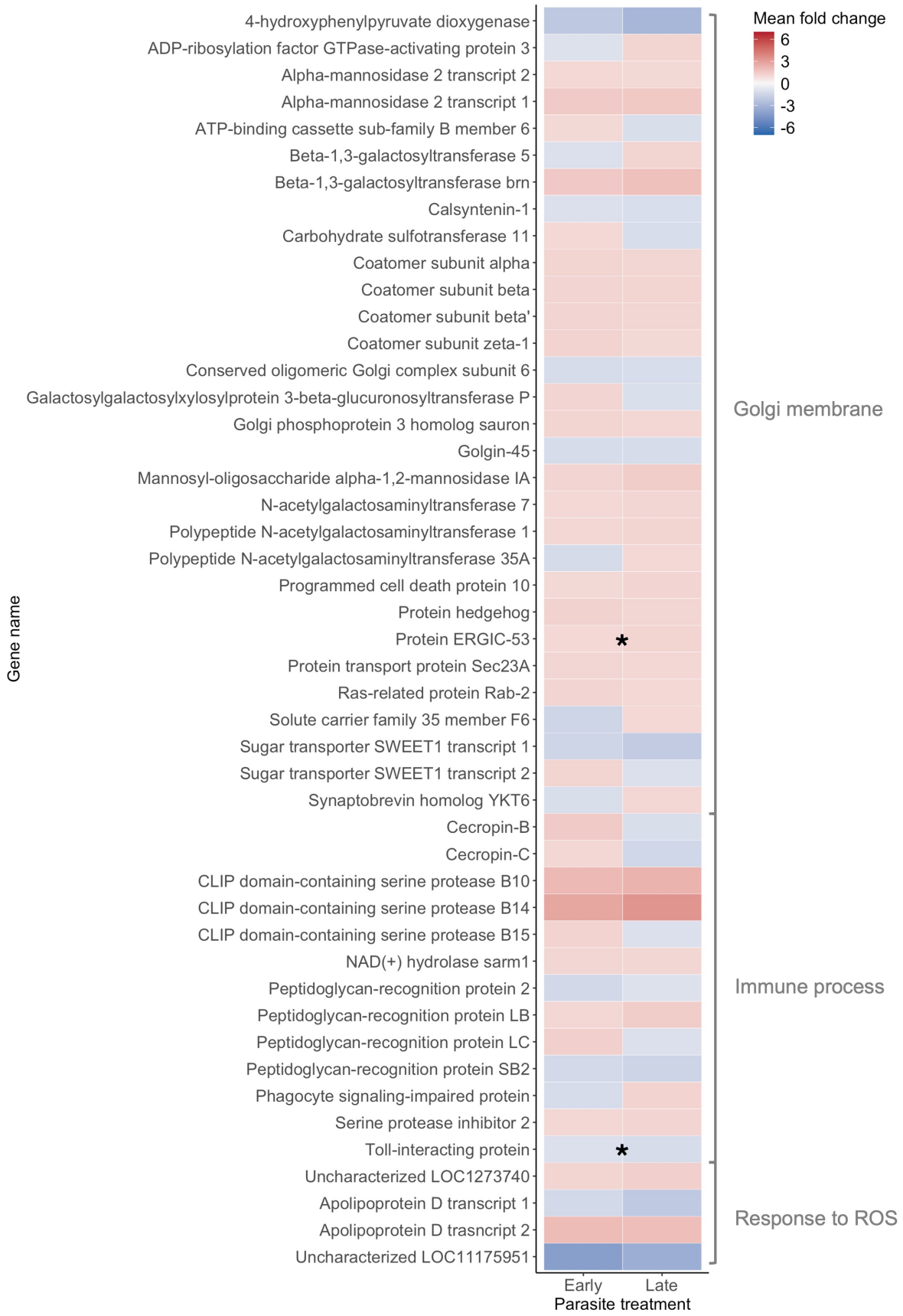
Mean fold change
6
3
0
-3
-6
4-hydroxyphenylpyruvate dioxygenase
ADP-ribosylation factor GTPase-activating protein 3
Alpha-mannosidase 2 transcript 2
Alpha-mannosidase 2 transcript 1
ATP-binding cassette sub-family B member 6
Beta-1,3-galactosyltransferase 5
Beta-1,3-galactosyltransferase brn
Calsyntenin-1
Carbohydrate sulfotransferase 11
Coatomer subunit alpha
Coatomer subunit beta
Coatomer subunit beta'
Coatomer subunit zeta-1
Conserved oligomeric Golgi complex subunit 6
Galactosylgalactosylxylosylprotein 3-beta-glucuronosyltransferase P
Golgi phosphoprotein 3 homolog sauron
Golgin-45
Mannosyl-oligosaccharide alpha-1,2-mannosidase IA
N-acetylgalactosaminyltransferase 7
Polypeptide N-acetylgalactosaminyltransferase 1
Polypeptide N-acetylgalactosaminyltransferase 35A
Programmed cell death protein 10
Protein hedgehog
Protein ERGIC-53
Protein transport protein Sec23A
Ras-related protein Rab-2
Solute carrier family 35 member F6
Sugar transporter SWEET1 transcript 1
Sugar transporter SWEET1 transcript 2
Synaptobrevin homolog YKT6
Cecropin-B
Cecropin-C
CLIP domain-containing serine protease B10
CLIP domain-containing serine protease B14
CLIP domain-containing serine protease B15
NAD(+) hydrolase sarm1
Peptidoglycan-recognition protein 2
Peptidoglycan-recognition protein LB
Peptidoglycan-recognition protein LC
Peptidoglycan-recognition protein SB2
Phagocyte signaling-impaired protein
Serine protease inhibitor 2
Toll-interacting protein
Uncharacterized LOC1273740
Apolipoprotein D transcript 1
Apolipoprotein D trasncript 2
Uncharacterized LOC11175951
Gene name
Golgi membrane
Immune process
Response to ROS
Early
Late
Parasite treatment

175

176 **Figure 4. Differentially host expressed candidate genes during infection with selected parasites.**
177 Fold difference in host expression of Golgi membrane (GO:0000139), response to reactive oxygen
178 species (GO:0000302) and immune system process (GO:0002376) markers when compared to
179 infection with the *Stock*. *Early* and *Late* selected fold change parasites was then compared to each
180 other using a linear model (see materials and methods for details). Although the expression of all
181 genes presented differed from the infection with *Stock* parasite, only the Toll-interacting and ERGIC-
182 53 transcripts' fold change significantly differed between *Early* and *Late* parasites. *Late* had a lower
183 expression of *Toll-interacting protein* ($df = 1$, $F = 9.70$, $p = 0.01$) and *protein ERGIC-53* ($df = 1$, $F =$
184 7.69, $p = 0.02$) than *Early* parasites, represented by an asterisk.

185

186 **Results (814)**

187 In this study, *A. gambiae* transcriptome in response to unselected and selected lines of the
188 microsporidian parasite *V. culicis* was characterized through RNA-seq. The findings suggest infection
189 by each parasite treatment resulted in distinct transcriptomic profiles, which differed in their host
190 immune response to each parasite. Moreover, the involvement of several biological processes, namely
191 Golgi apparatus-associated signalling and response to reactive oxygen species (ROS) were also
192 observed. The following sections describe and discuss these and other findings in detail.

193 Transcriptional profiles were measured on day 10 of mosquito adulthood, as a previous study has
194 identified this as the time when all *V. culicis* within the infected mosquitoes reach 100% prevalence in
195 spore production, regardless of the *V. culicis* line infecting them [25]. Hence, this time point was
196 chosen as sporulation represents an increase in parasite numbers and, therefore, should elicit a more
197 evident host response to the parasite. Nevertheless, it is noteworthy that, on average, infection by
198 different lines of the parasite reached 100% prevalence at slightly different days of adulthood - i.e.,
199 *Stock* at day 10, *Early* at day 8 and *Late* at day 4.

200 Across the twelve samples (i.e., one *Uninfected*, one *Stock,* infected with unselected *V. culicis*, five
201 *Early*, infected by five selection replicates for early transmission, and five *Late*, infected by five
202 selection replicates for late transmission), 20 to 38 million reads were obtained, covering over 9,900
203 genes. The reads were successfully aligned to the *A. gambiae* genome (SI Fig. S1), and quality control
204 confirmed their validity (SI Fig. S2). The number of genes detected by regime, selection, and
205 technical replicates can be found in the SI Table S1.

206 First, the host transcriptional profile of *A. gambiae* infected with the *Stock* parasite was compared to
207 *Uninfected* controls (Fig. 2, Table 1). Out of the 9,900 annotated genes, 863 (8.7%) were significantly
208 down-regulated, 1104 (11.1%) were significantly up-regulated, and 7953 (80.2%) showed no
209 differential expression (DE). A complete list of the transcripts for this comparison can be found in SI

210 Files S1-S11. Next, the focus turned to comparing to *Uninfected* controls. The 20 most up- and down-
211 regulated transcripts are listed in Table 1.

212 For this comparison, although a higher number of up-regulated genes was found, the down-regulated
213 genes exhibited higher fold changes. For instance, the most down-regulated gene was the *Putative*
214 *uncharacterized protein DDB_G0271606*, with a negative fold change of 1680.95. In contrast, the
215 most up-regulated gene was an uncharacterized gene with a positive fold change of 13.30.

216 Next, the DE profiles of *A. gambiae* infected by *Early* and *Late* parasite lines were also analyzed and
217 compared to *Stock* (Fig. 3). A heatmap showing the expression of all transcripts across the different
218 parasite lines shows a high fold-change in selected parasites (i.e., *Early* and *Late*) compared to a
219 standard infection by the *Stock* (even when this is compared to the *Uninfected* treatment) (Fig. 3a).
220 Overall, Figure 3a demonstrates distinct expression profiles across the different parasite treatments.
221 After comparing transcript expression to the reference *Stock*, transcripts that were uniquely DE in
222 each selected treatment and those shared between treatments were identified (Fig. 3bc).

223 For down-regulated genes, 81 genes were poorly expressed by *Early* parasites. In comparison, 71
224 genes were down-regulated by *Late* parasites, with 28 genes commonly down-regulated in both
225 treatments (Fig. 3b). For up-regulated genes, 113 genes were up-regulated in *Early* parasites,
226 compared to 52 in *Late* parasites, with 77 genes commonly up-regulated in both groups (Fig. 3c).
227 These findings suggest that a higher number of DE genes are found in response to infection by *Early*
228 parasites compared to late-selected ones, at least during the 10th day of host adulthood. However, a
229 notable overlap exists between both treatments (Fig. 3bc).

230 After categorizing the DE genes into their respective biological processes using Gene Ontology (GO)
231 categories, a heatmap was plotted to show the mean fold-change for each GO category across parasite
232 treatments (Fig. 3d). Most categories exhibited similar fold changes between *Early* and *Late* parasites.
233 However, three categories stood out as potential candidates for explaining differences between the
234 two selected treatments due to their distinct expression patterns and biological relevance: response to
235 reactive oxygen species (ROS), Golgi membrane, and immune system processes.

236 Genes with DE and their respective fold-change relative to the *Stock* were plotted for each candidate
237 GO category (Fig. 4). The Golgi membrane category had the highest number of DE genes and showed
238 the greatest variation between *Early* and *Late* parasites, followed by the immune process and response
239 to ROS categories. Fold-change differences between the selected treatments were also compared.
240 Only two genes showed significant differences: *Protein ERGIC-53* ($df = 1$, $F = 7.69$, $p = 0.02$; Golgi
241 membrane) and *Toll-interacting protein* ($df = 1$, $F = 9.70$, $p = 0.01$; Immune process). Both genes had
242 a higher fold change in *Late* parasites than in *Early* ones. However, while *Protein ERGIC-53* was up-
243 regulated, *Toll-interacting protein* was down-regulated (Fig. 4).

Discussion (1799)

The aim of this study is to provide a brief foundational description of the *A. gambiae* response to the microsporidian parasite *V. culicis*. To accomplish this, the host response was described and discuss in respect to infection by: i) an unselected microsporidian *V. culicis* (*Stock*), as well as ii) differently selected lines of the same microsporidian species, five selected for early transmission (*Early*) and five for late transmission (*Late*) within the same mosquito host (Fig. 1). The findings discussed below provide key insights into this host-parasite interaction and might have consequences for this vector's competence upon co-infection with *Plasmodium spp*.

1. Mosquito response to infection with unselected Stock of V. culicis

When the host's transcriptomic response to infection by *Stock* was compared (Fig. 2, Table 1), a large number of differentially expressed (DE) genes were observed (see File S2 for the complete list of transcripts and respective expression). Such a broad response has been reported in the mosquito *Aedes aegypti* when infected with *V. culicis* [33]. Nevertheless, only a small fraction of the host genome was DE, with unclassified genes leading the numbers, followed by genes associated with biological and cellular processes and several other metabolic gene ontology categories (Fig. 2). Overall, metabolic and biosynthetic processes were some of the most well-represented, which likely suggests changes in the transcriptional response linked to the energy processing and translation of immune- and non-immune elements. From the immunity-related elements, only a few DE markers were identified, with two being notably over-expressed: *Cecropin-B*, an antimicrobial peptide known for its fungicidal properties *in vitro* [36, 37], and *Ninjurin-2*, a non-apoptotic cell death protein induced by the Toll pathway and which plays a key role in the dipteran response to microbial infections [38, 39].

Significant over-expression of regeneration markers was also detected. For instance, *Annulin* was found to be responsible for peritrophic matrix formation in the gut and early resilience to infection [40], and *Obstructor-E*, a member of a multigene family, was shown to regulate insect cuticle development [41]. Additionally, *Rab11*, essential for circulatory iron internalization, was over-expressed [42], further validating previous findings on the role of iron during infection with *V. culicis*, where iron sequestration by the parasite has been hypothesized [43].

An overall down-regulation of sensory genes was observed, including *Prestin*, which increases gut pH [44] and *CIMAP1D*, involved in sound-sensory function [45]. *Arginine kinase 1*, known to participate in ATP-to-ADP conversion and consequent energy release in certain bacteria [46], was found to be severely down-regulated in infected mosquitoes (Table 1). Interestingly, most Mucin proteins were up-regulated, except for *Mucin-6*, which was down-regulated. Mucin proteins are recognized for their

277 role in epithelial lubrification, immune modulation and inflammation [47, 48]. Notably, *Mucin-6* is
278 exclusive to the *A. gambiae* gut, which protects against parasites such as *Plasmodium spp* [49].

279 ***2. Mosquito response to infection by selected lines of V. culicis***

280 Next, the focus is turned to infections caused by parasite lines that have undergone selection for early
281 or late transmission within *A. gambiae* [25] (Fig. 3 and 4). As expected, fewer genes were responsible
282 for differences between selected and unselected parasites, i.e., 299 for *Early* and 228 for *Late* (Fig.
283 3cd), than *Stock* and *Uninfected*, i.e., 1967 genes. Notably, a broader transcriptional response was
284 induced by *Early* parasites than by *Late* ones (when they are compared to the *Stock*), as indicated by
285 the high number of DE genes in both selection treatments (Fig. 3cd). Despite this, a core set of genes
286 was found to be commonly up- or down-regulated across both parasite treatments (Fig. 3bc).

287 To better understand the differences in transcriptomic profiles from infections with selected parasites,
288 DE genes were categorized into biological processes using GO analysis (Fig. 3d). Most of the
289 differences between *Early* and *Late* parasites were grouped into three GO biological processes: Golgi
290 membrane, immune processes, and response to reactive oxygen species (ROS). These findings are
291 unsurprising, given the biological relevance of these categories for infection [50–52], particularly
292 from the host's perspective. Equally interestingly, the distinct host transcriptomic profile observed in
293 response to infection between the *Early* and *Late* parasites indicates that selection did affect not only
294 phenotypic traits, as shown in previous studies [25, 29, 43], but also drove significant parasite
295 evolution, causing a substantial shift in the host's response to the selected parasites (Fig. 3 and 4).

296 The three GO categories were treated as candidate categories, along with their associated genes,
297 which are believed to play crucial roles in modulating host-parasite dynamics and therefore warrant
298 further study (Fig. 4). First, the Golgi membrane was considered, as it has recently gained attention
299 for its critical role in innate immune signalling, preceding other organelles such as mitochondria and
300 the endoplasmic reticulum (ER) during infection [50]. As a result, the apparent difference observed in
301 the host response to *Early* or *Late* parasite treatments was unsurprising (Fig. 3). The genes associated
302 with the Golgi membrane include coatomers, galactosyltransferases, and mannosidases, which are
303 involved in vesicle transport and carbohydrate metabolism with the ER. The richness and differential
304 expression of Golgi membrane-associated genes suggest that some upregulation of effectors involved
305 in glycosylation and trafficking processes in the Golgi apparatus occurs across both parasite
306 treatments (Fig. 4). One gene, *ERGIC-53*, stood out due to its significantly different fold-change
307 between host responses to infections by *Early* and *Late* parasites. The protein encoded by *ERGIC-53*
308 is involved in glycoprotein trafficking. The *Early* parasites seem to induce higher production of
309 ERGIC-53 and, consequently, this suggests an increased investment in glycoprotein trafficking
310 compared to *Late* (Fig. 4). Although the precise role of ERGIC-53 in the immune response of *A.*
311 *gambiae* remains unclear, it can be hypothesized, based on existing literature, that glycoproteins (e.g.,

312 peptidoglycan recognition proteins or PGRPs) serve as essential information markers for the host,
313 vital for accurate recognition and elimination of parasites [53, 54]. Nevertheless, it is important to
314 mention further studies have to be conducted to validate such claims. Statistical changes in these
315 effectors do not mean they are themselves involved in the process/changes but instead might be the
316 pathway they are in.

317 Second, variation in the expression of immune-related genes was analyzed, including *peptidoglycan-*
318 *recognition proteins* (PGRPs), *CLIP domain serine proteases* and *cecropins*, among others (Fig. 3). A
319 notable difference was observed between the host response to *Early* and *Late* parasite treatments, with
320 many of the DE immune related-genes being downregulated upon infection with *Late* parasites (Fig.
321 3). Interestingly, both *cecropin-B* and *cecropin-C* were overexpressed in response to early-selected
322 parasites compared to *Stock*, suggesting a more robust antimicrobial response. However, this pattern
323 was not observed in response to *Late* parasites, but rather the opposite. In particular, *CLIP domain*
324 *serine proteases* have been associated with mosquito late resistance to *Plasmodium* via melanisation
325 [55, 56] (Table 1, Fig. 4). In this study, I noticed all lines of *V. culicis* induced an up-regulation of
326 these immune effectors, suggesting that infection by this microsporidian might elicit an immune
327 response that has collateral damage to *Plasmodium* development.

328 Although it was hypothesized that the immune response to *Late* parasites would be stronger due to
329 their higher virulence, time, and replication within the host, the data might suggest otherwise. Two
330 hypotheses are proposed to explain this finding, although they are merely speculative at this stage.

331 The first hypothesis involves the recognition of *V. culicis* as a virulent parasite. As discussed in the
332 manuscript, *Early* parasites induce a larger Golgi membrane response, potentially leading to better
333 recognition of PGRPs than infection by Late parasites. This could explain the rapid up-regulation of
334 immune markers in response to *Early* parasites. The second hypothesis concerns the balance between
335 the costs and benefits of the immune response and its association with the presence/absence of
336 damage-associated molecular patterns (DAMPs) [57]. As with any other life history trait, investment
337 in immunity is expected to trade off with other physiological traits [58]. As suggested by Rolff and
338 Lazzaro (2012), the type of intensity of the immune response may result from the recognition of a
339 combination of molecules, alerting the host to the parasite (PGRPs) and/or to the damage inflicted by
340 the infection (DAMPs). If so, infection by the more virulent *Late* parasite could lead to a more costly
341 and damaging infection, potentially overwhelming the host. In this scenario, the host may prioritize
342 reproductive fitness over survival, which aligns with previous observations of increased reproductive
343 investment during infection by *Late* parasites [25]. This phenomenon has been documented in various
344 infections as predicted by life history theory [58]. In extreme cases, the investment shift to fecundity
345 can be lifelong due to a shortening of the host's survival. In this specific case, we refer to this
346 phenomenon as terminal investment, which may occur when a host invests its resources into fecundity

347 due to an inability to survive the infection [59–61]. It is unclear if this shift in fecundity and immunity
348 is temporary or observed throughout the host life, given that both fecundity and RNA-seq were
349 performed for the same infection time point and did not represent the whole infection process. It is
350 noteworthy to say the individuals in this study were not blood-fed, necessary for their reproduction.
351 Although we cannot confirm there is a trade-off with fecundity or other life history traits, we are
352 aware *A. gambiae* invests in its first clutch of eggs before having a blood meal, which would represent
353 at least a partial investment in fecundity. Moreover, from this category, the *Toll-interacting protein*
354 was found to have significantly different fold changes between the infection by each of the two
355 selection parasite treatments (Fig. 4). This gene, which produces a protein important for parasite
356 recognition [62–65], was slightly more up-regulated in response to *Early* parasites than to *Late* ones
357 (Fig. 4). This might support the idea that *Early* parasites may be more recognizable by the host's
358 immune system. However, the extent to which parasite selection has affected the presence or absence
359 of specific PGRPs that enable host recognition remains unclear.

360 It is essential to state the limitations of this study at this stage. Here, the aim is to provide the first
361 description of the mosquito response to *V. culicis* and, potentially, other microsporidia by extension.
362 However, the observations in this study are insufficient to fully understand parasite evolution, nor do
363 they reflect in-depth mechanisms or how they change with the progression of infection, which is
364 particularly difficult in the presence of multiple lines of *V. culicis* with distinct growing cycles.
365 Nevertheless, discussing the potential scenarios is of interest and might pave research avenues for
366 future studies.

367 Third, only a few genes were found to be DE in response to ROS, showing mixed expression patterns
368 (Fig. 4). Overall, *Early* parasites elicited a stronger host response to ROS than *Late* ones, suggesting
369 higher oxidative stress within the host. This is likely due to a heightened immune response to this
370 infection treatment.

371

372 Conclusions (447)

373 In conclusion, the transcriptional response of *A. gambiae* to infection by *V. culicis* has revealed
374 curious and significant insights into this host-parasite interaction and its evolutionary history.
375 Moreover, the findings in this study further explain many of the results measured in previous studies
376 concerning the effects of selecting *V. culicis* for early and late transmission [25, 29, 43]. Differential
377 expression of genes related to immune response, Golgi membrane function, and oxidative stress were
378 observed, with distinct patterns emerging between infections with reference to *Stock*, *Early* and *Late*
379 parasite lines. Overall, *Early* parasites seemed to elicit a broader and more apparent immune response,
380 characterized by the upregulation of immune-related genes such as cecropin and PGRPs and enhanced

381 glycoprotein trafficking through the Golgi apparatus. In contrast, *Late* parasites appeared to trigger a
382 weaker immune response and, therefore, potentially evolved immune evasion mechanisms - but such
383 claims are still up for testing.

384 Altogether, the results of this study demonstrate that selection pressures on *V. culicis* not only
385 influence its phenotypic traits but also drive significant changes in the host gene expression, revealing
386 complex host-parasite co-evolutionary dynamics. Further investigation is needed to elucidate and
387 quantify the specific molecular mechanisms involved, particularly in relation to immune strategies
388 and the balance between host survival and reproductive fitness. Additionally, it is important to
389 position this study within the context of the microsporidian's ability to interfere with *Plasmodium*
390 development, as previously mentioned. Vector-borne parasites, such as *Plasmodium spp.*, transmitted
391 by this host, have long transmission cycles within their vectors. It is reasonable to expect that co-
392 infection of Plasmodium spp. and microsporidia may inadvertently select for late-transmitted
393 microsporidian parasites, which could have significant consequences for the spread of both parasites
394 within a population. Although the mechanism by which microsporidians suppress *Plasmodium*
395 development remains unclear, our study demonstrated that melanisation-based immunity is
396 upregulated, which might facilitate late collateral melanisation of *Plasmodium* oocysts. Nevertheless,
397 this hypothesis is still up for testing, as beside *CLIP proteases*, we observed a limited immune
398 response that could impact *Plasmodium spp.* and hence, resource competition between the parasites
399 might be a main source of this inhibitory relationship too. Moreover, although conclusions have to be
400 taken with some consideration, the results suggest a lack of immunity towards late-transmitted *V.*
401 *culicis* might highlight the potential of this parasite as a biological vector-control as it suggests
402 selection to reduce its prevalence in a population is low. Further research is required to understand
403 this interaction fully, but our study stands as a foundation for them. These findings provide valuable
404 insights that could inform future vector control strategies, particularly in the context of the
405 evolutionary pressures exerted by parasites on mosquito populations and the diseases they vector.

406

407 # Materials and Methods (1063)

408 ***1. Experimental model***

409 The Kisumu strain of the mosquito host *Anopheles gambiae (s.s.)* and evolved lines of the
410 microsporidian parasite *Vavraia culicis floridensis* were used for these experiments. These parasite
411 lines had previously been selected for seven generations for: i) early transmission and shorter time
412 within the host (i.e., *Early*); or for ii) late transmission and longer time within the host (i.e., *Late*); or
413 iii) they come from an unselected reference, our unselected laboratory stock (i.e., *Stock*) [25]. Further
414 details on the selection experiment and its maintenance are described in Silva and Koella (2024). All

415 experiments and rearing were conducted under standard laboratory conditions (26 ± 1ºC, 70 ± 5%
416 relative humidity, and 12 h light/dark).

417 ***2. Experiment and samples collection***

418 Freshly hatched *A. gambiae* larvae were reared in groups of 50 individuals per petri dish (120 mm
419 diameter × 17 mm) containing 80 ml of distilled water. Larvae were fed daily with Tetramin Baby
420 fish food according to their age: 0.04, 0.06, 0.08, 0.16, 0.32, and 0.6 mg/larva for 0, 1, 2, 3, 4, and 5
421 days or older, respectively. On the second day of larval development, individuals were exposed to
422 10,000 spores per larva of their respective *V. culicis* treatment, or not exposed in the case of the
423 *Uninfected* treatment. At pupation, individuals were transferred into 50 ml falcon tubes with
424 approximately 10 ml of distilled water and were allowed to emerge as adults. Female mosquitoes
425 were transferred to individual cups with humid filter paper and given a constant 6% sucrose solution
426 until death. On day 10 of adulthood, all live female mosquitoes were collected, snap-frozen in liquid
427 nitrogen, and stored at -80ºC until RNA extraction. Transcriptomic profiles were assessed at day 10 of
428 adulthood, as previous studies on these lines have shown this to be when all hosts produce infective
429 spores [25]. Thus, a stronger host response and more pronounced signatures of parasite selection were
430 anticipated for this time point.

431 ***3. RNA extractions***

432 RNA extractions were performed using Qiagen's RNAeasy Universal Plus kit following the provided
433 protocol. Before beginning the protocol, ten female mosquitoes per treatment were pooled in a 1.5 mL
434 microcentrifuge tube with 1000 µl of Qiazol reagent (from the RNAeasy Universal Plus kit by
435 Qiagen) briefly mixed, and two stainless steel beads (Ø 2 mm) were added. Each tube was
436 homogenized using a Qiagen TissueLyser LT at a frequency of 30 Hz for three minutes. The Qiagen
437 kit protocol was then followed, resulting in a 50 µl eluted solution of RNA in nuclease-free water at a
438 concentration of approximately 300 ng/µl for each treatment. RNA samples were standardized to 10
439 ng/µl and delivered on dry ice to the Genomic Technologies Facility (University of Lausanne,
440 Switzerland) for further processing, as described below.

441 ***4. RNA sequencing***

442 RNA quality was assessed using a Fragment analyzer (Agilent Technologies). The poly-A tails and
443 adapters were removed from single-end reads, and quality was trimmed with Cutadapt version 4.8
444 [66]. Reads matching ribosomal RNA sequences were removed with fastq_screen version 0.11.1 [67].
445 Reads longer than 40nt were aligned against the concatenated genomes of *Anopheles gambiae* (NCBI:
446 GCA_943734735.2) and *Vavraia culicis floridensis* (NCBI: GCA_000192795.1) using STAR version
447 2.7.10a [68]. The number of read counts per gene locus was summarized with htseq-count version
448 0.11.2 [69] using gene annotation. RNA-seq libraries were prepared from 250 ng of total RNA with

449 the Illumina Stranded mRNA Prep reagents (Illumina) using a unique dual indexing strategy and
450 following the official protocol, which was automated on a Sciclone liquid handling robot
451 (PerkinElmer). Libraries were quantified by a fluorometric method (QubIT, Life Technologies), and
452 their quality was assessed on a Fragment Analyzer (Agilent Technologies). Sequencing was
453 performed on an Illumina NovaSeq 6000 for 150 cycles single read. Sequencing data were
454 demultiplexed using the bcl2fastq2 Conversion Software (version 2.20, Illumina).

455 ***5. Statistical analysis***

456 All the analyses were performed with R version 4.3.0. in RStudio version 3034.06.2+561. The
457 following packages were used for the statistical analysis and diagnosis, and for visualising and
458 plotting the data: "Glimma" [70], "cowplot" [71], "ggrepel" [72], "RColorBrewer" [73], "maptools"
459 [74], "sp" [75], "edgeR" [76], "MASS" [77], "limma" [78], "knitr" [79], "ggplot2" [80] and "dplyr"
460 [81]. Figure panels were created and edited with BioRender.com and Microsoft PowerPoint 16.16.27.

461 The high quality of the RNA-seq data alignment was verified using RSeQC version 5.0.1 [82].
462 Alignment rates to both genomes exceed 93.5% for all samples (SI Fig. S1a). A very few number of
463 reads aligned to *V. culicis*, ranging from 127 to 5,393 (SI Fig. S1b). *A. gambiae* samples exhibit good
464 sequencing depth (SI Fig. S1c) and diverse gene representation. The gene body coverage is biased
465 towards the 3' end, suggesting partial RNA degradation, but this pattern is consistent across all
466 samples.

467 Genes with low counts were filtered out according to the rule of 3 count(s) per million (cpm) in at
468 least 4 sample(s). Library sizes were scaled using TMM normalization and log-transformed into
469 counts per million or CPM (EdgeR package version 3.42.4) [76]. Statistical quality controls were
470 performed through density gene expression distribution, clustering, and sample PCA (SI Fig. S2).
471 Differential expression was computed with limma-trend approach [78] by fitting all samples into one
472 linear model. Next, the following group of comparisons were performed:

473 - Infected with *Stock vs. Uninfected* (1 comparison).

474 - Infected with selected parasite *vs.* infected with *Stock* (10 comparisons, one for each parasite
475 line).

476 A moderated t-test was used for each contrast. The Benjamini-Hochberg method computed an
477 adjusted p-value for each comparison, controlling for false discovery rate (FDR, Adj. p). Then, a host
478 gene ontology (GO) enrichment analysis was carried out on differentially expressed (DE) genes
479 through Panther 19.0 [illegible] and "vectorbase.org" using the *A. gambiae* genome as a reference (Fig. 2-4).
480 The host response to different biological replicate lines of *Early* and *Late* were then pooled together
481 per selection regime, and their average expression, compared to *Stock*, was calculated and plotted.

Afterwards, a candidate gene analysis was performed (Fig. 4) taking into account the differently expressed biological processes in selected parasites, comparatively to *Stock* (Fig. 3). For each DE transcript of the GO:0000139 (Golgi membrane), GO:0000302 (Response to reactive oxygen species) and GO:0002376 (Immune system process) classes, a linear model was run with fold-change as a dependent variable and parasite treatment as an explanatory variable. These comparisons allow us to test for differential fold change (compared to *Stock*) for *Early* and *Late* parasites.

Author contributions

LMS designed and conducted the experiments, analyzed the data and wrote the manuscript.

Acknowledgements

I thank Tiago G. Zeferino, Paula Escuer Pifarré, and Amjad Khalaf for their advice and experimental support. I also thank the Lausanne Genomic Technologies Facility (University of Lausanne, Switzerland) team, Johann Weber, Julien Marquis, Sandra Calderon Copete, and Viviane Praz for the library preparation, sequencing, and data analysis. I especially thank Jacob C. Koella for constant feedback, support, and critical comments on the first draft of the manuscript. The project was supported by the Basler Stiftung für biologische Forschung and LMS by SNF grant 310030_192786.

Competing interests

The author declare that they have no competing interests.

References

[1] Silva LM, Acerbi G, Amann M, et al. Exposure to Pseudomonas spp. increases Anopheles gambiae insecticide resistance in a host-dependent manner. *Sci Rep* 2024; 14: 29789.

[2] Ranasinghe HAK, Amarasinghe LD. Naturally occurring microbiota associated with mosquito breeding habitats and their effects on mosquito larvae. *Biomed Res Int*; 2020.

[3] Dong Y, Manfredini F, Dimopoulos G. Implication of the mosquito midgut microbiota in the defense against malaria parasites. *PLoS Pathog* 2009; 5: e1000423.

[4] Caragata EP, Tikhe C V, Dimopoulos G. Curious entanglements: interactions between

512 mosquitoes, their microbiota, and arboviruses. *Curr Opin Virol* 2019; 37: 26–36.
513 [5] Duncan AB, Agnew P, Noel V, et al. The consequences of co-infections for parasite
514 transmission in the mosquito A edes aegypti. *J Anim Ecol* 2015; 84: 498–508.
515 [6] Bozic J, Capone A, Pediconi D, et al. Mosquitoes can harbour yeasts of clinical significance
516 and contribute to their environmental dissemination. *Environ Microbiol Rep* 2017; 9: 642–648.
517 [7] Becnel JJ, Weiss LM. *Microsporidia: pathogens of opportunity*. John Wiley & Sons
518 Incorporated, 2014.
519 [8] Herren JK, Mbaisi L, Mararo E, et al. A microsporidian impairs Plasmodium falciparum
520 transmission in Anopheles arabiensis mosquitoes. *Nat Commun* 2020; 11: 1–10.
521 [9] Bjørnson S, Oi D. Microsporidia biological control agents and pathogens of beneficial insects.
522 *Microsporidia Pathog Oppor* 2014; 635–670.
523 [10] Franzen C. Microsporidia: a review of 150 years of research. *Open Parasitol J*; 2.
524 [11] Seatamanoch N, Kongdachalert S, Sunantaraporn S, et al. Microsporidia, a highly adaptive
525 organism and its host expansion to humans. *Front Cell Infect Microbiol* 2022; 12: 924007.
526 [12] Keeling PJ, Fast NM, Law JS, et al. Comparative genomics of microsporidia. *Folia Parasitol*
527 *(Praha)* 2013; 52: 8–14.
528 [13] Keesey IW, Koerte S, Khallaf MA, et al. Pathogenic bacteria enhance dispersal through
529 alteration of Drosophila social communication. *Nat Commun* 2017; 8: 265.
530 [14] Keeling PJ, Fast NM. Microsporidia: biology and evolution of highly reduced intracellular
531 parasites. *Annu Rev Microbiol* 2002; 56: 93–116.
532 [15] Silva LM, Zeferino TG, Koella JC. Vavraia culicis. *Trends Parasitol*. Epub ahead
533 of print 25 March 2025. DOI: 10.1016/j.pt.2025.02.011.
534 [16] Koella JC, Saddler A, Karacs TPS. Blocking the evolution of insecticide-resistant malaria
535 vectors with a microsporidian. *Evol Appl* 2012; 5: 283–292.
536 [17] Koella JC, Lorenz L, Bargielowski I. Microsporidians as evolution-proof agents of malaria
537 control? *Adv Parasitol* 2009; 68: 315–327.
538 [18] Bargielowski I, Koella JC. A possible mechanism for the suppression of Plasmodium berghei
539 development in the mosquito Anopheles gambiae by the microsporidian Vavraia culicis. *PLoS*
540 *One* 2009; 4: e4676.
541 [19] Kelly JF, Anthony DW, Dillard CR. A laboratory evaluation of the microsporidian Vavraia
542 culicis as an agent for mosquito control. *J Invertebr Pathol* 1981; 37: 117–122.
543 [20] Lorenz LM, Koella JC. The microsporidian parasite Vavraia culicis as a potential late life–
544 acting control agent of malaria. *Evol Appl* 2011; 4: 783–790.
545 [21] Vyas-Patel N. The Suppression of Plasmodium berghei in Anopheles coluzzii infected later
546 with Vavraia culicis. *bioRxiv* 2023; 2002–2023.
547 [22] Makhulu EE, Onchuru TO, Gichuhi J, et al. Localization and tissue tropism of the symbiont
548 Microsporidia MB in the germ line and somatic tissues of Anopheles arabiensis. *MBio* 2024;

549 15: e02192-23.
550 [23] Bukhari T, Pevsner R, Herren JK. Microsporidia: a promising vector control tool for residual
551 malaria transmission. *Front Trop Dis* 2022; 3: 957109.
552 [24] Zeferino TG, Koella JC. Host-specific effects of a generalist parasite of mosquitoes. *Sci Rep*
553 2024; 14: 18365.
554 [25] Silva LM, Koella JC. Complex interactions in the life cycle of a simple parasite shape the
555 evolution of virulence. *bioRxiv* 2024; 2024.01.28.577571.
556 [26] Sy VE, Agnew P, Sidobre C, et al. Reduced survival and reproductive success generates
557 selection pressure for the dengue mosquito Aedes aegypti to evolve resistance against
558 infection by the microsporidian parasite Vavraia culicis. *Evol Appl* 2014; 7: 468–479.
559 [27] Vyas-Patel N. Anopheles coluzzii infection by the microsporidian, Vavraia culicis: the effect
560 of host age. *bioRxiv* 2020; 2010–2020.
561 [28] Khalaf A, Francis O, Blaxter ML. Genome evolution in intracellular parasites: Microsporidia
562 and Apicomplexa. *J Eukaryot Microbiol* 2024; e13033.
563 [29] Silva LM, Koella JC. Virulence evolution: thinking outside of the host. *bioRxiv* 2024; 2005–
564 2024.
565 [30] Nakjang S, Williams TA, Heinz E, et al. Reduction and expansion in microsporidian genome
566 evolution: new insights from comparative genomics. *Genome Biol Evol* 2013; 5: 2285–2303.
567 [31] Yassine H, Osta MA. Anopheles gambiae innate immunity. *Cell Microbiol* 2010; 12: 1–9.
568 [32] Osta MA, Christophides GK, Vlachou D, et al. Innate immunity in the malaria vector
569 Anopheles gambiae: comparative and functional genomics. *J Exp Biol* 2004; 207: 2551–2563.
570 [33] Desjardins CA, Sanscrainte ND, Goldberg JM, et al. Contrasting host–pathogen interactions
571 and genome evolution in two generalist and specialist microsporidian pathogens of
572 mosquitoes. *Nat Commun* 2015; 6: 7121.
573 [34] Kanost MR, Jiang H. Clip-domain serine proteases as immune factors in insect hemolymph.
574 *Curr Opin insect Sci* 2015; 11: 47–55.
575 [35] Waterhouse RM, Kriventseva E V, Meister S, et al. Evolutionary dynamics of immune-related
576 genes and pathways in disease-vector mosquitoes. *Science (80-)* 2007; 316: 1738–1743.
577 [36] De Lucca AJ, Bland JM, Jacks TJ, et al. Fungicidal and binding properties of the natural
578 peptides cecropin B and dermaseptin. *Med Mycol* 1998; 36: 291–298.
579 [37] De Lucca AJ, Bland JM, Vigo CB, et al. D-cecropin B: proteolytic resistance, lethality for
580 pathogenic fungi and binding properties. *Med Mycol* 2000; 38: 301–308.
581 [38] Broderick S, Wang X, Simms N, et al. Drosophila Ninjurin A induces nonapoptotic cell death.
582 [39] Thomas T, De T Das, Sharma P, et al. Structural and functional prediction analysis of
583 mosquito Ninjurin protein: Implication in the innate immune responses in Anopheles
584 stephensi. *Int J Mosq Res* 2014; 1: 60–65.
585 [40] Wang Z, Wilhelmsson C, Hyrsl P, et al. Pathogen entrapment by transglutaminase—a

586 conserved early innate immune mechanism. *PLoS Pathog* 2010; 6: e1000763.
587 [41] Behr M, Hoch M. Identification of the novel evolutionary conserved obstructor multigene
588 family in invertebrates. *FEBS Lett* 2005; 579: 6827–6833.
589 [42] Wilcke M, Johannes L, Galli T, et al. Rab11 regulates the compartmentalization of early
590 endosomes required for efficient transport from early endosomes to the trans-golgi network. *J*
591 *Cell Biol* 2000; 151: 1207–1220.
592 [43] Silva LM, Vallat A, Koella JC. Mechanisms of host exploitation by a microsporidian parasite.
593 *bioRxiv*; 2024–12. Epub ahead of print 2024. DOI: https://doi.org/10.1101/2024.12.13.628237.
594 [44] Hirata T, Czapar A, Brin L, et al. Ion and solute transport by Prestin in Drosophila and
595 Anopheles. *J Insect Physiol* 2012; 58: 563–569.
596 [45] Senthilan PR, Piepenbrock D, Ovezmyradov G, et al. Drosophila auditory organ genes and
597 genetic hearing defects. *Cell* 2012; 150: 1042–1054.
598 [46] Cozzone AJ. ATP-dependent protein kinases in bacteria. *J Cell Biochem* 1993; 51: 7–13.
599 [47] Dam TK, Brewer CF. Multivalent lectin—carbohydrate interactions: energetics and
600 mechanisms of binding. *Adv Carbohydr Chem Biochem* 2010; 63: 139–164.
601 [48] Kufe DW. Mucins in cancer: function, prognosis and therapy. *Nat Rev Cancer* 2009; 9: 874–
602 885.
603 [49] Shen Z, Dimopoulos G, Kafatos FC, et al. A cell surface mucin specifically expressed in the
604 midgut of the malaria mosquito Anopheles gambiae. *Proc Natl Acad Sci* 1999; 96: 5610–5615.
605 [50] Tao Y, Yang Y, Zhou R, et al. Golgi apparatus: an emerging platform for innate immunity.
606 *Trends Cell Biol* 2020; 30: 467–477.
607 [51] Bahia AC, Oliveira JHM, Kubota MS, et al. The role of reactive oxygen species in Anopheles
608 aquasalis response to Plasmodium vivax infection. *PLoS One* 2013; 8: e57014.
609 [52] Andreyev AY, Kushnareva YE, Starkova NN, et al. Metabolic ROS signaling: to immunity
610 and beyond. *Biochem* 2020; 85: 1650–1667.
611 [53] Davicino RC, Eliçabe RJ, Di Genaro MS, et al. Coupling pathogen recognition to innate
612 immunity through glycan-dependent mechanisms. *Int Immunopharmacol* 2011; 11: 1457–
613 1463.
614 [54] Sperandio M, Gleissner CA, Ley K. Glycosylation in immune cell trafficking. *Immunol Rev*
615 2009; 230: 97–113.
616 [55] Zhang X, Li M, El Moussawi L, et al. CLIPB10 is a terminal protease in the regulatory
617 network that controls melanization in the African malaria mosquito Anopheles gambiae. *Front*
618 *Cell Infect Microbiol* 2021; 10: 585986.
619 [56] Zeineddine S, Jaber S, Saab SA, et al. Late sporogonic stages of Plasmodium parasites are
620 susceptible to the melanization response in Anopheles gambiae mosquitoes. *Front Cell Infect*
621 *Microbiol*; 14. Epub ahead of print 1 August 2024. DOI: 10.3389/fcimb.2024.1438019.
622 [57] Lazzaro BP, Rolff J. Danger, microbes, and homeostasis. *Science (80-)* 2011; 332: 43–44.

623 [58] Stearns SC. Trade-offs in life-history evolution. *Funct Ecol* 1989; 3: 259–268.
624 [59] Hudson AL, Moatt JP, Vale PF. Terminal investment strategies following infection are
625 dependent on diet. *J Evol Biol* 2020; 33: 309–317.
626 [60] Clutton-Brock TH. Reproductive effort and terminal investment in iteroparous animals. *Am*
627 *Nat* 1984; 123: 212–229.
628 [61] Duffield KR, Bowers EK, Sakaluk SK, et al. A dynamic threshold model for terminal
629 investment. *Behav Ecol Sociobiol* 2017; 71: 1–17.
630 [62] Burns K, Clatworthy J, Martin L, et al. Tollip, a new component of the IL-1RI pathway, links
631 IRAK to the IL-1 receptor. *Nat Cell Biol* 2000; 2: 346–351.
632 [63] Zhang G, Ghosh S. Negative regulation of toll-like receptor-mediated signaling by Tollip. *J*
633 *Biol Chem* 2002; 277: 7059–7065.
634 [64] Didierlaurent A, Brissoni B, Velin D, et al. Tollip regulates proinflammatory responses to
635 interleukin-1 and lipopolysaccharide. *Mol Cell Biol*.
636 [65] Valanne S, Wang J-H, Rämet M. The Drosophila toll signaling pathway. *J Immunol* 2011;
637 186: 649–656.
638 [66] Martin M. Cutadapt removes adapter sequences from high-throughput sequencing reads.
639 *EMBnet J* 2011; 17: 10–12.
640 [67] Wingett SW, Andrews S. FastQ Screen: A tool for multi-genome mapping and quality control.
641 *F1000Research*; 7.
642 [68] Dobin A, Davis CA, Schlesinger F, et al. STAR: ultrafast universal RNA-seq aligner.
643 *Bioinformatics* 2013; 29: 15–21.
644 [69] Anders S, Pyl PT, Huber W. HTSeq—a Python framework to work with high-throughput
645 sequencing data. *bioinformatics* 2015; 31: 166–169.
646 [70] Su S, Law CW, Ah-Cann C, et al. Glimma: interactive graphics for gene expression analysis.
647 *Bioinformatics* 2017; 33: 2050–2052.
648 [71] Wilke CO, Wickham H, Wilke MCO. Package 'cowplot'. *Streamlined plot theme plot Annot*
649 *'ggplot2*; 1.
650 [72] Slowikowski K, Schep A, Hughes S, et al. Package ggrepel. *Autom position non-overlapping*
651 *text labels with 'ggplot2*.
652 [73] Neuwirth E, Neuwirth ME. *Package 'RColorBrewer'*. CRAN 2011-06-17 08: 34: 00. Apache
653 License 2.0, 2011.
654 [74] Bivand R, Lewin-Koh N, Pebesma E, et al. Package 'maptools'. *Packag 'maptools'*.
655 [75] Pebesma E, Bivand R, Pebesma ME, et al. Package 'sp'. *Compr R Arch Netw*; 9.
656 [76] Robinson MD, McCarthy DJ, Smyth GK. edgeR: a Bioconductor package for differential
657 expression analysis of digital gene expression data. *bioinformatics* 2010; 26: 139–140.
658 [77] Ripley B, Venables B, Bates DM, et al. Package 'mass'. *Cran r* 2013; 538: 113–120.
659 [78] Ritchie ME, Phipson B, Wu DI, et al. limma powers differential expression analyses for RNA-

660 sequencing and microarray studies. *Nucleic Acids Res* 2015; 43: e47–e47.
661 [79] Xie Y. knitr: a comprehensive tool for reproducible research in R. In: *Implementing*
662 *reproducible research*. Chapman and Hall/CRC, 2018, pp. 3–31.
663 [80] Wickham H. *ggplot2: elegant graphics for data analysis*. springer, 2016.
664 [81] Wickham H, François R, Henry L, et al. Package 'dplyr'. *A Gramm Data Manip R Packag*
665 *version*; 8.
666 [82] Wang L, Wang S, Li W. RSeQC: quality control of RNA-seq experiments. *Bioinformatics*
667 2012; 28: 2184–2185.
668

669 # Supplementary information

670

671 **Table S1.** Number of genes annotated per sample.
672 **Figure S1.** Host RNA-sequencing and parasite gene counts.
673 **Figure S2.** Quality control clustering and PCAs.
674 **Figure S3.** Heatmap of the complete host transcriptome in response to each parasite treatment and
675 replicate.
676 **File S1.** Transcript expression and statistical contrasts for *Stock* infection *vs. Uninfected*.
677 **File S2.** Transcript expression and statistical contrasts for *Early* (selection replicate 1) infection *vs.*
678 *Stock* infection..
679 **File S3.** Transcript expression and statistical contrasts *Early* (selection replicate 2) infection *vs. Stock*
680 infection.
681 **File S4.** Transcript expression and statistical contrasts for *Early* (selection replicate 3) infection *vs.*
682 *Stock* infection.
683 **File S5.** Transcript expression and statistical contrasts for *Early* (selection replicate 4) infection *vs.*
684 *Stock* infection.
685 **File S6.** Transcript expression and statistical contrasts for *Early* (selection replicate 5) infection *vs.*
686 *Stock* infection.
687 **File S7.** Transcript expression and statistical contrasts for *Late* (selection replicate 1) infection *vs.*
688 *Stock* infection.
689 **File S8.** Transcript expression and statistical contrasts for *Late* (selection replicate 2) infection *vs.*
690 *Stock* infection.
691 **File S9.** Transcript expression and statistical contrasts for *Late* (selection replicate 3) infection *vs.*
692 *Stock* infection.
693 **File S10.** Transcript expression and statistical contrasts for *Late* (selection replicate 4) infection *vs.*
694 *Stock* infection.
695 **File S11.** Transcript expression and statistical contrasts for *Late* (selection replicate 5) infection *vs.*

696 *Stock* infection.